Molecular Crystals and Liquid Crystals Science and Technology. Section A. Molecular Crystals and Liquid Crystals

Publication details, including instructions for authors and subscription information:
http://www.tandfonline.com/loi/gmcl19

Bipolar Electrodiffusion Model for Electroconvection in Nematics

Martin Treiber [a] & Lorenz Kramer [a]

[a] Physikalisches Institut, Universität Bayreuth, 95440, Bayreuth, Germany

Version of record first published: 23 Sep 2006.

To cite this article: Martin Treiber & Lorenz Kramer (1995): Bipolar Electrodiffusion Model for Electroconvection in Nematics, Molecular Crystals and Liquid Crystals Science and Technology. Section A. Molecular Crystals and Liquid Crystals, 261:1, 311-326

To link to this article: http://dx.doi.org/10.1080/10587259508033478

Mol. Cryst. Liq. Cryst. 1995, Vol. 261, pp. 311–326
Reprints available directly from the publisher
Photocopying permitted by license only

BIPOLAR ELECTRODIFFUSION MODEL FOR ELECTROCONVECTION IN NEMATICS

MARTIN TREIBER AND LORENZ KRAMER
Physikalisches Institut, Universität Bayreuth, 95440 Bayreuth, Germany

Abstract The common description of the electrical behavior of a nematic liquid crystal as an anisotropic dielectric medium with (weak) ohmic conductivity is extended to an electrodiffusion model with two active ionic species. Under appropriate, but rather general conditions the additional effects can lead to a distinctive change of the threshold behavior of the electrohydrodynamic instability, namely to travelling patterns instead of static ones. This may explain the experimentally observed phenomena.

1. INTRODUCTION

In the last years electrohydrodynamic convection (EHC) in nematic liquid crystals (NLC) has become a standard physical phenomenon for investigating pattern formation and the paradigma for anisotropic systems [1, 2, 3, 4]. The main advantage of EHC compared to other pattern-forming systems are the short time scales, the possibility to make cells with very large aspect ratios and two easily adjustable control parameters (AC voltage V_{eff} and frequency ω_{ext}), leading to a wealth of instability scenarios [3, 4]. For a planar (homogeneous) alignment of the director at the confining plates (electrodes), one observes at the instability from the unstructured state (primary instability) normal or oblique rolls, i.e. roll axis normal or tilted with respect to the equilibrium director [1]. Both patterns can be stationary or travelling [5, 6, 7, 8, 9]; furthermore the bifurcation can be continuous or (very weakly) hysteretic [10].

The scenario appearing above threshold depends on ω_{ext}, the thickness d of the cell, the material and the temperature. Especially the conductivity (a material parameter easily adjustable by doping), the dielectric anisotropy and, as will be shown below, other electrical properties of the material are relevant.

The commonly used theory to describe EHC are the Ericksen-Leslie equations [11, 12] combined with the quasi-static Maxwell equations, thereafter referred to as the standard model [1]. This theory describes quantitatively (in many cases) the stationary features like the threshold voltage, the wavenumber of the rolls and the transition from normal to oblique

rolls in particular for sufficiently low external frequencies (conductive regime). The main discrepancy between the predictions of the standard model and the experiments, however, is the observed Hopf bifurcation. The linear analysis leads for a planar configuration always to a continuous bifurcation to stationary rolls [1]. It is even difficult to produce with this model a primary Hopf bifurcation by changing rather drastically some material parameters [2]. The discrepancies are pronounced for thin cells, pure materials (low conductivity) and high external frequencies.

In this work we replace in the electrical part of the standard model the ohmic conductivity by two dynamically active species of charge carriers (one positive, one negative). The constant ohmic conductivity of the standard model becomes a dynamical variable on its own with Ohm's law replaced by migration and diffusion parts of the current. Together with the charge density ρ (coupled to the potential of the induced field via the Poisson equation) the new model contains two electrical variables. The new physical processes incorporated in the theory are ionic migration, diffusion and dissociation-recombination. The corresponding new material parameters are mobilities, diffusion constants and a recombination rate constant. The associated time and length scales are, respectively, the migration time τ_{mig} needed for an ion to travel through the cell, the (Debye) diffusion length λ_D and the (linear) recombination time τ_{rec}. If τ_{rec} is much smaller than the other time scales the conductivity can be eliminated and one has ρ as the only electrical dynamic variable. If in addition τ_{mig} is large and λ_D is small, drift and diffusion can be neglected and we are back to ohmic conductivity and the standard model. Comparing $\tau_{rec} \propto 1/n_0$ (n_0 = equilibrium density of charge carriers of each species) and $\tau_{mig} \propto d^2/V_{eff}$ with the director relaxation time $\tau_d \propto d^2$, and $\lambda_D \propto n_0^{-1/2}$ with the roll dimensions, it is evident, that our model differs from the standard model just in the parameter ranges where the latter fails to describe the experiments.

In Sec. 2 we present the basic equations and assumptions. In Sec. 3 the model is applied to the basic state and linearized around this state. Secion 4 contains an approximate calculation showing a Hopf bifurcation for sufficiently thin cells, clean materials or sufficiently high external frequencies (for materials with negative dielectric anisotropy). Sec. 5 gives a discussion and a brief comparison with experimental results.

2. BASIC EQUATIONS

It seems reasonable to assume that the conductivity of NLC's is caused by two species of ionic charge carriers arising from dissociation of impurities or of the NLC itself [13]. We assume charges $\pm e$ (no loss of generality) and overall neutrality $\int d^3\underline{r} n^+ = \int d^3\underline{r} n^-$ with the number densities n^+ and n^-. The electrical current $\underline{J}^\pm$ of each species is caused by migration in the electrical fields $\underline{E}$, diffusion due to carrier-density gradients, and advection with the fluid velocity $\underline{v}$, $\underline{J} = \underline{J}^+ + \underline{J}^-$ with $\underline{J}^\pm = \underline{J}^\pm_{mig} + \underline{J}^\pm_{diff} + \underline{J}^\pm_{adv}$ [14]. In uniaxial-anisotropic systems we have

$$\underline{J}_{mig} = e(\underline{\underline{\mu}}^+ n^+ + \underline{\underline{\mu}}^- n^-)\underline{E} =: \underline{\underline{\sigma}}\,\underline{E}, \tag{1}$$

$$\underline{J}_{diff} = -e(\underline{\underline{D}}^+ \underline{\nabla} n^+ - \underline{\underline{D}}^- \underline{\nabla} n^-), \tag{2}$$

$$\underline{J}_{adv} = e(n^+ - n^-)\underline{v} =: \rho \underline{v}, \tag{3}$$

where ρ is the charge density and $\underline{\underline{\sigma}}$ the tensor of the local conductivity. The mobility tensors are $\mu^\pm_{ij} = \mu^\pm_\perp \delta_{ij} + \mu^\pm_a n_i n_j$ ($\underline{n}$ is the director field) with $\mu^\pm_\perp, \mu^\pm_a$ essentially independent of n^+, n^- and $\underline{E}$ [13]. We assume that the relative anisotropies for the two ionic species are the same and thus equal to the relative conductivity anisotropy, $\sigma_a/\sigma_\perp$, as measured in the low-field ohmic range,

$$\mu^\pm_{ij} = \mu^\pm_\perp(\delta_{ij} + \frac{\sigma_a}{\sigma_\perp} n_i n_j) =: \mu^\pm_\perp \sigma'_{ij}. \tag{4}$$

We adopt the Einstein law

$$\underline{\underline{D}}^\pm = V_T \underline{\underline{\mu}}^\pm, \tag{5}$$

where $V_T = k_B T/e \approx 26\text{mV}$ is the thermal potential. Experimentally this relation is satisfied within a factor of about 3 [15, 16, 18].

The dissociation-recombination process $AB \rightleftharpoons A^+ + B^-$ with the undissociated molecules or impurities AB and the ions A^+, B^- [13] is described in homogeneous systems (no spatial variation) by the rate equations $\dot{n}^\pm = k_d n_{AB} - k_r n^+ n^-$ (k_d, k_r =dissociation and recombination constants) and $\dot{n}_{AB} = -\dot{n}^\pm$. In the weak-dissociation limit $n^+,\ n^- << n_{AB}$ the concentration n_{AB} of the undissociated molecules is nearly constant in time, and can be replaced by its equilibrium value which we write as $K_{diss} n^{eq}_{AB} = n_0^2$, where $K_{diss} = k_d/k_r$ is the dissociation constant and n_0 is the equilibrium value of n^+ and n^-. This assumption is usually valid when $K_{diss} << n_0$. For MBBA with ionic dopant TBATPB Ref. [13] gives $K_{diss} = 3.4 \times 10^{21} m^{-3}$ while equilibrium densities $n_0 = \sigma_{eq}/(e(\mu^+ + \mu^-))$ are of the order of $10^{19} m^{-3}$ for typical mobility and conductivity values (Tables I and II).

TABLE I Scaling

quantity	scaling unit	typical value +
lengths	d/π	$\pi^{-1}(10...100\mu\text{m})$
time	$\tau_d^{(0)} = \frac{\gamma_1 d^2}{K_{eff}\pi^2}$	0.073 s $\left(\frac{d}{10\mu m}\right)^2$
voltage	$V_c^{(0)} = \sqrt{\frac{\pi^2 K_{eff}}{\sigma_a \tau_q}}$	2.7 V
conductivities	$\sigma_{eq} = \mu e n_0$	$10^{-7}...10^{-9}(\Omega\text{m})^{-1}$
dependent quantities E and ρ	$\frac{V_c^{(0)}\pi}{d}$ and $\frac{V_c^{(0)}\epsilon_0\epsilon_\perp\pi^2}{d^2}$	
orientational elasticities	$K_{eff} = K_{11} + K_{33}$	15.3×10^{-12}N
dielectric constants	$\epsilon_0\epsilon_\perp$	4.2×10^{-11}As/Vm
viscosities	$\gamma_1 = \alpha_3 - \alpha_2$	0.11 kg m s^{-1}

+ parameter set MBBA I [1]

TABLE II material parameters related to conduction

parameter	material	value and source
mobility μ *	MBBA	0.371 [13]; 1 [14]
	5CB	0.06...0.35 [16, 17, 18]
mobility ratio γ	MBBA**	1 [13]
	5CB	$<< 1$ [18]
mobility anisotropy $\frac{\mu_a}{\mu_\perp} = \frac{\sigma_a}{\sigma_\perp}$	MBBA	0.33 [13]; 0.5 [21]
recombination-	5CB	$10\text{s}^{-1}n_0^{-1}$ [17]
rate constant k_r	dielectric liquids	$10^{15}\text{m}^3\text{s}^{-1}$ [14];
dissociation constant K_{diss}	MBBA**	$3.4 \times 10^{21}\text{m}^{-3}$ [13]

* in units of $10^{-9}m^2/(Vs)$ ** Doping TBATPB.

In the spatially extended case the rate equations are generalized to

$$\partial_t n^\pm \pm \frac{1}{e}\underline{\nabla}\cdot\underline{J}^\pm = \dot{n}^\pm, \tag{6}$$

or with (1) - (5) and $n_{AB} = n_{AB}^{eq}$

$$\partial_t n^\pm + \underline{\nabla}\cdot\left[\underline{v}n^\pm + \mu_\perp^\pm \underline{\underline{g}}'(\pm\underline{E} - V_T\underline{\nabla})n^\pm\right] = k_r(n_0^2 - n^+n^-). \tag{7}$$

In view of coupling Eqs.(7) to the director and momentum-balance equations it is convenient to write Eqs.(7) as a continuity equation for the charge density $\rho = e(n^+ - n^-)$ and

a balance equation for the conductivity $\sigma := \sigma_\perp = e(\mu_\perp^+ n^+ + \mu_\perp^- n^-)$,

$$\partial_t \rho + \underline{\nabla} \cdot \left[\rho \underline{v} + \underline{\underline{\sigma}}' \underline{E} \sigma - V_T \underline{\underline{\sigma}}' \underline{\nabla} \left(d(\gamma)\sigma + 2\mu s_1(\gamma)\rho\right)\right] = 0, \tag{8}$$

$$\partial_t \sigma + \underline{\nabla} \cdot \left[\sigma \underline{v} + \mu \underline{\underline{\sigma}}' \underline{E}(d(\gamma)\sigma + \mu s_1(\gamma)\rho) - \mu V_T \underline{\underline{\sigma}}' \underline{\nabla} \left(s_2(\gamma)\sigma + d(\gamma)\mu s_1(\gamma)\rho\right)\right]$$
$$= k_r n_0 \sigma_{eq} \left[1 - \frac{(\sigma + \mu_- \rho)(\sigma - \mu_+ \rho)}{\sigma_{eq}^2}\right], \tag{9}$$

where we introduced the effective mobility $\mu = \mu_\perp^+ + \mu_\perp^-$, the mobility ratio $\gamma = \mu_\perp^-/\mu_\perp^+$ together with $d(\gamma) = (1-\gamma)/(1+\gamma)$, $s_1(\gamma) = \gamma/(1+\gamma)^2$ and $s_2(\gamma) = (1+\gamma^2)/(1+\gamma)^2$, and the equilibrium conductivity $\sigma_{eq} = \mu e n_0$. With the Poisson equation

$$\rho = \underline{\nabla} \cdot (\epsilon_0 \epsilon_\perp \underline{\underline{\epsilon}}' \underline{E}), \quad \underline{\underline{\epsilon}}' = \delta_{ij} + \frac{\epsilon_a}{\epsilon_\perp} n_i n_j \tag{10}$$

and the potential for $\underline{E}$ (see Sec. 3) all electrical variables are given in terms of the (scalar) potential and σ.

We need five boundary conditions (BCs) for the electrical variables in addition to the usual no-slip planar BCs $\underline{n} = (1,0,0), \underline{v} = 0$ at the confining plates ($z = \pm d/2$), which act as electrodes (NLC layer of infinite extent in the x-y plane) . The applied voltage is given by

$$\int_{-d/2}^{d/2} dz \; E_z = V(t). \tag{11}$$

Furthermore there are relations between current, electrical field and density for each species at the electrodes which can depend in a complicated way on electrochemical processes and may be parametrised e.g. for $z = d/2$ as $J_z^\pm = \sigma_{surface}^\pm E_z - D_{surface}^\pm (n_{ext}^\pm - n^\pm)$. Two limiting cases are i) strongly injecting electrodes, i.e. at least one $\sigma_{surface}$ is very large, which leads to $E_z = 0$ (space-charge limiting conditions) and is (in the isotropic-unipolar case) adopted e.g. in Refs [14, 19] and ii) no transfer of any charge through the electrodes (blocking electrodes),

$$J_z^+(z = \pm d/2) = J_z^-(z = \pm d/2) = 0. \tag{12}$$

These last BCs do not involve unknown electrochemical processes and will be assumed in the rest of this paper. Blocking electrodes imply that the averaged charge density per area, $Q := lim_{A\to\infty} \frac{1}{A} \int_A dx \; dy \int_{-d/2}^{d/2} dz \rho$ or, equivalently, $E(d/2) - E(-d/2)$ is constant and we can incorporate permanently adsorbed charges (for future purpose) by setting $Q = Q_{ad} + \int dz \rho = 0$ or with the Poisson equation (10)

$$E_z(d/2) - E_z(-d/2) = -\frac{Q_{ad}}{\epsilon_0 \epsilon_\perp}. \tag{13}$$

Equations (8)and (9) together with the director and momentum balance, and incompressibility equations of the standard model [1], the boundary conditions (11),(12) and the charge adsorption (13), determining the conserved quantity $E_z(d/2) - E_z(-d/2)$ represent the bipolar electrodiffusion model. It contains in addition to $\sigma_\perp$ and σ_a three more conduction parameters $\mu_\perp^+, \gamma$ and k_r of the NLC at a given temperature (see Table II). Equations (8) and (9) are coupled to the fluid velocity by the advection term and to the director by $\underline{\underline{\varrho}}'$ and $\underline{\underline{\epsilon}}'$. Conversely, the director and momentum-balance equations of the standard model are coupled to the electrical fields via the electrical torque $\propto \epsilon_0 \epsilon_a (\underline{n} \cdot \underline{E})\underline{E}$ on the director and the electrical volume force $\underline{\nabla}\,\underline{\underline{T}}^{el} = \rho \underline{E} + h.o.t.$ on the fluid. The director and momentum-balance equations do not couple directly to σ.

To see the relative magnitude and time scales of the different processes we scale all variables and parameters according to Table I. The result is

$$P_1(\partial_t + \underline{v}\cdot\underline{\nabla})\rho = -\underline{\nabla}\cdot\underline{\underline{\varrho}}'\underline{E}\sigma + D\underline{\nabla}\cdot\underline{\underline{\varrho}}'\underline{\nabla}\left[\alpha^{-1}d(\gamma)\sigma + 2s_1(\gamma)\rho\right], \tag{14}$$

$$\begin{aligned} P_1(\partial_t + \underline{v}\cdot\underline{\nabla})\sigma &= -\alpha\underline{\nabla}\cdot\underline{\underline{\varrho}}'\underline{E}\left[d(\gamma)\sigma + \alpha s_1(\gamma)\rho\right] + D\underline{\nabla}\cdot\underline{\underline{\varrho}}'\underline{\nabla}\left[s_2(\gamma)\sigma + d(\gamma)\alpha s_1(\gamma)\rho\right] \\ &\quad - r\left[\left(\sigma + \frac{\gamma\alpha}{1+\gamma}\rho\right)\left(\sigma - \frac{\alpha}{1+\gamma}\rho\right) - 1\right], \end{aligned} \tag{15}$$

$$\underline{\nabla}\cdot\underline{\underline{\epsilon}}'\underline{E} = \rho, \tag{16}$$

and scaled director and momentum-balance equations (eqs.(52) in [20] with a slightly different scaling). The BCs for an applied voltage $V(t) = \sqrt{2}V_{eff}\cos\omega_{ext}t$ and blocking electrodes are

$$\begin{aligned} \int_{-\pi/2}^{\pi/2} dz\; E_z &= V'(t), \\ \left[E_z\sigma - D\partial_z(\alpha^{-1}d(\gamma)\sigma + 2s_1(\gamma)\rho)\right]_{z=\pm 1/2} &= 0, \\ \left[D\partial_z\sigma - \alpha E_z(d(\gamma)\sigma + 2\alpha s_1(\gamma)\rho)\right]_{z=\pm 1/2} &= 0, \end{aligned} \tag{17}$$

where the scaled voltage is $V'(t) = V(t)/V_c^{(0)} = \sqrt{2R}\cos\omega t$, and we wrote (12) as $J_z^+ \pm J_z^- = 0$.

Apart from the two external control parameters R and ω_0 the model contains four system parameters P_1, α, r and D, see Table III. The first three are (Prandtl-number like) time-scale ratios relating the time scales of director relaxation, charge relaxation, carrier-generation-recombination kinetics and carrier migration, and D is (up to a factor $\sqrt{2}$) the diffusion length (Debye screening length) $\lambda_D = (\mu V_T \tau_q/2)^{1/2}$ in units of d/π. The diffusion is not an independent parameter since it is coupled to α via the scaled Einstein law $D = \alpha V_T/V_c^{(0)}$.

TABLE III System parameters of the bipolar model

parameter	physical process	typical value#	proportionality
$\sqrt{R} = \frac{V_{eff}}{V_c^{(0)}}$	control parameter	≥ 2.5	
$\omega_0 = \omega_{ext}\tau_d^{(0)}$	control parameter	$1...P_1^{-1}$	
$P_1 = \frac{\tau_q}{\tau_d^{(0)}} = \frac{\epsilon_0\epsilon_\perp}{\sigma_\perp \tau_d^{(0)}}$	charge relaxation	0.057	$(\sigma_\perp d^2)^{-1}$
$\alpha = \frac{\tau_q}{\tau_{mig}(V_c^{(0)})} = \mu V_c^{(0)} \tau_q \frac{\pi^2}{d^2}$	ion migration	1.1	$\frac{V_c^{(0)}}{n_0 d^2} = \frac{\mu e V_c^{(0)}}{\sigma_\perp d^2}$
$r = \frac{\tau_q}{2\tau_{rec}} = k_r n_0 \tau_q$	recombination	≤ 1	$\frac{k_r n_0}{\sigma_\perp} = \frac{k_r}{\mu e}$
$\sqrt{D} = \sqrt{2}\pi\frac{\lambda_D}{d} = \frac{\pi}{d}\sqrt{\frac{V_T \epsilon_0 \epsilon_\perp}{e n_0}}$	diffusion	0.1	$(n_0 d^2)^{-1/2} \propto \alpha^{1/2}$

parameter set MBBA I with
$\sigma_\perp = 10^{-8}(\Omega\mathrm{m})^{-1}, \mu = 10^{-9} m^2/(Vs)$, $d = 10\mu$m, and $\gamma = 1$.

The standard theory is recovered when $\sigma - \sigma_{eq}$ remains negligibly small (and diffusion can be neglected). This is the case when i) the recombination time $\tau_{rec} = (2k_r n_0)^{-1}$ is much smaller than the charge relaxation time and ii) the ion migration time to travel through the cell at the applied voltage is much larger than the charge relaxation time and the time scale of the external frequency. This essentially means $r >> 1$ and $\alpha << 1$, see Table III.

3. BASIC STATE AND LINEAR ANALYSIS

In contrast to the standard model the electrodiffusion model actually implies a nontrivial basic state $\sigma_0(z,t)$, $\delta\rho_0(z,t)$, $\underline{E}_0 = (0,0,E_0(z,t))$, $\underline{n}_0 = (1,0,0)$ and $\underline{v}_0 = 0$. For blocking electrodes this is obvious because charge conservation together with finite conductivity leads to an accumulation of charges near the electrodes. Other BCs lead to a nontrivial basic state (for the electrical variables) as well, except ohmic BCs, $J_z = \sigma_\perp E_z$, implicitely assumed in the standard model.

We decompose the fields of the scaled electrodiffusion model into (i) the basic state of the standard model, (ii) the difference between the actual basic state and the standard-model basic state (denoted with a δ), and (iii) linearized fluctuations,

$$\begin{aligned}
&\underline{n} = (1,0,0) + (0,n_y,n_z) + h.o.t.,\\
&\sigma \;= \sigma_0(z,t) + \tilde{\sigma}(\underline{r},t) \qquad = 1 + \delta\sigma_0(z,t) + \tilde{\sigma}(\underline{r},t),\\
&\underline{E} \;= E_0(z,t)\underline{e}_z - \underline{\nabla}\phi(\underline{r},t) \quad = (\pi^{-1}V'(t) + \delta\underline{E}_0(z,t))\underline{e}_z - \underline{\nabla}\phi(\underline{r},t),\\
&\rho \;= \delta\rho_0(z,t) + \tilde{\rho}(\underline{r},t) \qquad = \delta\rho_0(z,t) + \hat{\epsilon}\phi + \epsilon_a E_0 \partial_x n_z + h.o.t.,
\end{aligned} \tag{18}$$

where $\delta\rho_0 = \partial_z \delta E_0$, and we used (16), the second equation of (10) and the definition $\hat{\epsilon} = -\epsilon'_{ij}(\underline{n}_0)\partial_i\partial_j = -(\underline{\nabla}^2 + \epsilon_a\partial_x^2)$ to express $\bar{\rho}$ in terms of n_z and the induced potential ϕ.

Inserting the basic state into (14)-(16) and using $\partial_z E_0 = \delta\rho_0$ gives the basic-state equations in terms of E_0 and the deviations from the trivial basic state, $\delta\sigma_0, \delta\rho_0$,

$$P_1\partial_t\delta\rho_0 = \left[-1 + 2Ds_1(\gamma)\partial_z^2\right]\delta\rho_0 + \left[-E_0\partial_z + \alpha^{-1}Dd(\gamma)\partial_z^2\right]\delta\sigma_0 - \delta\rho_0\delta\sigma_0, \quad (19)$$

$$\begin{aligned} P_1\partial_t\delta\sigma_0 &= \alpha\left[(r-1)d(\gamma) - \alpha s_1(\gamma)E_0\partial_z + Dd(\gamma)\alpha s_1(\gamma)\partial_z^2\right]\delta\rho_0 \\ &- \left[2r + \alpha d(\gamma)E_0\partial_z - Ds_2(\gamma)\partial_z^2\right]\delta\sigma_0 \\ &- r\delta\sigma_0^2 + \alpha(r-1)d(\gamma)\delta\sigma_0\delta\rho_0 + \alpha^2(r-1)s_1(\gamma)\delta\rho_0^2. \end{aligned} \quad (20)$$

In regions where $\delta\rho_0 << 1$ and $\delta\sigma_0 << 1$ the volume charge relaxes with the rate τ_q^{-1} and diffuses with the effective diffusion constant $D_{eff}^{\rho\rho} = 2Ds_1(\gamma)d^2/\pi^2\tau_q = 4\lambda_D^2/\tau_q$. The deviation from the equilibrium conductivity relaxes with the rate $2r/\tau_q = 1/\tau_{rec}$, diffuses with the effective constant $D_{eff}^{\sigma\sigma} = Ds_2(\gamma)d^2/\pi^2\tau_q = 2s_2(\gamma)\lambda_D^2/\tau_q$ and is advected with the effective velocity $v_\sigma = \alpha d(\gamma)E_0 d/\pi\tau_q$. Both quantities are coupled by further relaxational, advective and diffusive terms. For equal mobilities ($\gamma = 1, d(\gamma) = 0$) only the diagonal relaxation and diffusion constants and the offdiagonal advective terms survive. The nonlinear terms $\propto \delta\sigma_0\delta\rho_0$ and $\propto \delta\sigma_0^2$ in (19) and (20) increase the respective relaxations by factors $1 + \delta\sigma_0$ and $1 + \delta\sigma_0/2$. The term $\propto \delta\rho_0^2$ contains the Coulomb repulsion [22] and a part of the nonlinear recombination. Equations (17) give the BCs for $\delta\rho_0$, $\sigma_0 = 1 + \delta\sigma_0$ and E_0.

Clearly, the trivial basic state is incompatible with the blocking BCs (17) because the BCs are not homogeneous in $\delta\rho_0$ and $\delta\sigma_0$. For 'ohmic' BCs $J_z = \sigma_{eq}E_z$ and $J_z^+ - J_z^- = e(\mu_\perp^+ - \mu_\perp^-)E_z$ the BCs (17) are homogeneous with σ_0 replaced by $\delta\sigma_0$ and the trivial basic state is a solution. For the blocking or other general BCs boundary layers of accumulated charge appear, which influence the impedance of the system. These effects will be discussed in future work. Here we assume that their influence on the stability of the basic state is small (see below).

The linearised equations of the electrodiffusion model are obtained by inserting the decomposition (18) into the scaled equations (14) and (15). The two electrical equations of the resulting set of equations for $\tilde{\rho}$ and $\tilde{\sigma}$ are (primes on the basic-state quantities denote z derivatives and $\hat{\sigma}$ is defined in analogy to $\hat{\epsilon}$)

$$
\begin{aligned}
P_1\partial_t(\hat{\epsilon}\phi \;+\; & \epsilon_a E_0 \partial_x n_z) \\
= \; & \left[-\sigma_0\hat{\sigma} + \sigma_0'\partial_z - 2Ds_1(\gamma)\hat{\sigma}\hat{\epsilon}\right]\phi - \left[E_0\partial_z + \delta\rho_0 + \alpha^{-1}Dd(\gamma)\hat{\sigma}\right]\tilde{\sigma} \qquad (21)\\
+ \; & \left\{-\sigma_a\sigma_0 E_0 + D\left[\alpha^{-1}d(\gamma)\sigma_a\sigma_0' + 2s_1(\gamma)(\sigma_a\delta\rho_0' - \hat{\sigma}\epsilon_a E_0)\right]\right\}\partial_x n_z - P_1\delta\rho_0' v_z, \\
P_1\partial_t\tilde{\sigma} = \; & \alpha\left\{-\alpha s_1(\gamma)\left[(E_0\hat{\epsilon} - \delta\rho_0')\partial_z + \delta\rho_0(\hat{\sigma} + \hat{\epsilon} + 2r\hat{\epsilon})\right]\right. \\
- \; & d(\gamma)\left[\sigma_0\hat{\sigma} - \sigma_0'\partial_z + Ds_1(\gamma)\hat{\sigma}\hat{\epsilon} - r\sigma_0\hat{\epsilon}\right]\Big\}\phi \\
- \; & \left[\alpha d(\gamma)(E_0\partial_z + \delta\rho_0(1-r)) + Ds_2(\gamma)\hat{\sigma} + 2r\sigma_0\right]\tilde{\sigma} \\
+ \; & \left\{\alpha d(\gamma)\left[-\sigma_0\sigma_a E_0 + Ds_1(\gamma)(\sigma_a\delta\rho_0' - \hat{\sigma}\epsilon_a E_0) + r\sigma_0\epsilon_a E_0\right]\right. \qquad (22)\\
+ \; & \left.\alpha^2 s_1(\gamma)E_0\left[-\delta\rho_0\sigma_a - \epsilon_a(2\delta\rho_0(1+r) + E_0\partial_z)\right] + Ds_2(\gamma)\sigma_a\sigma_0'\right\}\partial_x n_z - P_1\sigma_0' v_z,
\end{aligned}
$$

with the (homogeneous) BCs

$$[E_0 - \alpha^{-1}Dd(\gamma)\partial_z]\tilde{\sigma} + [\sigma_0 - 2Ds_1(\gamma)\partial_z^2]\tilde{E}_z = 0, \qquad (23)$$

$$[D\partial_z - \alpha E_0 d(\gamma)]\tilde{\sigma} - \alpha[d(\gamma)\sigma_0 + 2\alpha s_1(\gamma)(\delta\rho_0 + E_0\partial_z)]\tilde{E}_z = 0. \qquad (24)$$

Since for director modes $\partial_z \approx \pi/d$ and $D << 1$ the diffusive parts can be neglected leading to $\tilde{\sigma}/\tilde{E}_z = -\sigma_0/E_0$ and $(\delta\rho_0 + E_0\partial_z)\tilde{E}_z = 0$, which can be fulfilled by the BCs of the standard model $\partial_z\tilde{E}_z = \tilde{\rho} = 0$ for $\delta\rho_0 = 0$. The linearized director and momentum-balance equations of the standard model are changed by some terms from the nontrivial basic state. They are given (other scaling) in Ref. [1], Eqs. (3.2) with $V(t)$ replaced by $V(t) + \pi\delta E_0(z,t)$ and the volume-force term $\propto q\phi$ in (3.2e) (iq corresponds to ∂_x) supplemented by a contribution $\delta\rho_0'\epsilon_0 q\phi$.

For $\alpha \to 0$, $D \to 0$ and without the nontrivial parts of the basic state one has $\tilde{\sigma} \to 0$ and Eq. (21) reduces to $(P_1\partial_t\hat{\epsilon} + \hat{\sigma})\phi = -\pi^{-1}(P_1\epsilon_a\partial_t + \sigma_a)V'(t)\partial_x n_z$, the continuity equation (3.2a) in [1].

The BCs for $\delta\rho_0$, $\sigma_0 = 1 + \delta\sigma_0$ and E_0 are the same as (17). Neglecting the small field deviations δE_0 which are of the order of λ_D/d, $E_0 \approx \pi^{-1}V'(t)$ is spatially constant and the first two terms on the rhs. of (19) and (20) are linear in the deviations from the standard-model-basic state.

4. ANALYTICAL RESULTS IN A SIMPLE CASE

In this section we show that the linear equations (21) - (24) can lead to a Hopf bifurcation. We assume blocking BCs and boundary layers with a thickness much smaller

than the cell thickness and in the rest of the volume an essentially trivial basic state, i.e. we adopt $\sigma_0 = 1, \pi E_0(t) = V'(t) = \sqrt{2R}\cos\omega t$ and $\delta\rho_0 = 0$. Further we neglect diffusion and restrict ourselves to the normal-roll regime by setting $(\phi(\underline{r},t), \tilde{\sigma}(\underline{r},t), n_z(\underline{r},t)) = e^{iqx}(\overline{\phi}(z,t), \overline{\sigma}(z,t), \overline{n}_z(z,t))$ and $n_y = v_y = 0$. The fluid velocities v_x, v_z in the director equation for n_z are eliminated adiabatically. This is justified because the viscous relaxation time $\tau_{visc} = \rho_m d^2/(\alpha_4/2) \approx 10^{-5}$s is usually much shorter than the other relevant time scales [4, 20]. With these assumptions one obtains from (21), (22) and the director and fluid equations from the standard model

$$[P_1\partial_t\hat{\epsilon}_q + \hat{\sigma}_q]\overline{\phi} + E_0(t)\partial_z\overline{\sigma} + \left[P_1\epsilon_a(\dot{E}_0(t) + E_0(t)\partial_t) + \sigma_a E_0(t)\right] iq\overline{n}_z = 0, \quad (25)$$

$$\alpha\left[\alpha E_0(t)s_1(\gamma)\hat{\epsilon}_q\partial_z + d(\gamma)(\hat{\sigma}_q - r\hat{\epsilon}_q)\right]\overline{\phi} + [P_1\partial_t + \alpha d(\gamma)E_0(t)\partial_z + 2r]\,\overline{\sigma}$$
$$+\alpha E_0(t)\left[d(\gamma)(\sigma_a - r\epsilon_a) + \alpha s_1(\gamma)\epsilon_a E_0(t)\partial_z\right] iq\overline{n}_z = 0, \quad (26)$$

$$\frac{\hat{L}_{n\phi}}{\sigma_a}\pi^2 E_0(t)\overline{\phi} + \left[\partial_t - \hat{\lambda}_0 - \frac{\epsilon_a}{\sigma_a}\pi^2 E_0^2(t)\right] iq\overline{n}_z = 0, \quad (27)$$

where $\hat{\epsilon}_q = -\partial_z^2 + (1+\epsilon_a)q^2$, $\hat{\sigma}_q = -\partial_z^2 + (1+\sigma_a)q^2$ (the operators $\hat{\epsilon}$ and $\hat{\sigma}$ applied to the normal-roll state) and $\hat{K}_q = -\partial_z^2 + K_{33}q^2$. The zero-field director relaxation operator $\hat{\lambda}_0$ is given by [20]

$$\hat{\lambda}_0 = -\frac{\hat{K}_q}{K_{eff}}(1 - \hat{L}_{nn})^{-1}, \quad (28)$$

For simplicity the z-dependence of the velocity v_z is expressed already here in terms of a normalized Galerkin mode $f_v(z)$ which gives

$$\hat{L}_{n\phi} = \frac{\hat{\epsilon}_q - \epsilon_a L_{nn} q^2}{1 - L_{nn}}, \quad (29)$$

$$L_{nn} = q^4\left\{\int_{-\pi/2}^{\pi/2} dz\, f_v^*(z)\left[\frac{\alpha_4+\alpha_6}{2}(q^2 - \partial_z^2)^2 + q^2(q^2 - (1+\alpha_1)\partial_z^2)\right] f_v(z)\right\}^{-1} \quad (30)$$

with the anisotropic shear viscosities $\alpha_i, i = 1...6$ of the NLC. Some small terms $\propto \alpha_3$ have been omitted. The BCs (23), (24) without diffusion can be combined to give

$$\partial_z^2\overline{\phi} = 0, \quad \partial_z\overline{\phi} = E_0(t)\overline{\sigma}. \quad (31)$$

The first BC is consistent with the ansatz for the field inhomogeneity of the symmetric-conductive mode of the standard model (Type I A of [1, 2]). Since then $\partial_z\overline{\phi} \neq 0$, the second BC implies the conductivity perturbation to be nonzero at the boundaries, i.e the lowest-order mode of the conductivity is antisymmetric in z.

To get analytical results we use the lowest-order Galerkin ansatz for the symmetric-conductive director mode, $iq\overline{n}_z = n^{(0)}\cos kz, \overline{\phi} = (\phi^{(1)}e^{i\omega t} + \phi^{(-1)}e^{-i\omega t})\cos kz$, the antisymmetric mode for the conductivity $\overline{\sigma} = \sigma^{(0)}\sin kz$ to which the ϕ equation (25) couples

$n^{(0)}$ and $\phi^{(\pm 1)}$ via the $E_0\partial_z$ term, and the first Chandrasekhar function [1] for $f_v(z)$. The σ equation (26) couples at lowest order also to symmetric conductivity modes $\propto e^{\pm i\omega t}\cos kz$ but they do not satisfy the second BC (31). Inserting this ansatz into (25)-(27) one obtains four coupled equations for $n^{(0)}, \phi^{(-1)}, \phi^{(1)}$ and $\sigma^{(0)}$. Assuming for the charge relaxation rate $\tau_q^{-1} >> \tau_{rec}^{-1}, \tau_d^{-1}$ one can eliminate adiabatically the induced potentials $\phi^{(\pm 1)}$ and obtains a 2×2 system for the symmetric director/antisymmetric conductivity modes,

$$\begin{aligned} [\partial_t - \lambda_\sigma(R,\omega)]\,\sigma^{(0)} &+ \left[\frac{R\tilde{\alpha}^2(\sigma_a\frac{\epsilon_q}{\sigma_q} - \epsilon_a)}{1+\omega'^2}\right] n^{(0)} &= 0, \\ \left[-\frac{L_{n\phi}R}{(1+\omega'^2)\sigma_q\sigma_a}\right]\sigma^{(0)} &+ [\partial_t - \lambda_n(R,\omega)]\,n^{(0)} &= 0. \end{aligned} \tag{32}$$

The numbers $\epsilon_q, \sigma_q, K_q$ and λ_0 are the corresponding operators with $\partial_z^2 \to -1$. The normalized external frequency is $\omega' = \omega_{ext}\tau_q\epsilon_q/\sigma_q$, where ϵ_q/σ_qvaries typically from 0.6 to 0.9. The relaxation rates λ_σ and λ_n of the uncoupled σ mode and of the conductive director mode of the standard model are given by

$$\lambda_\sigma = -\left(\tilde{r} + \frac{R\tilde{\alpha}^2\epsilon_q}{(1+\omega'^2)\sigma_q}\right), \tag{33}$$

$$\lambda_n = \lambda_0 + R\left(\frac{L_{n\phi}}{(1+\omega'^2)\sigma_q} + \frac{\epsilon_a}{\sigma_a}\left(1 + \frac{\omega'^2 L_{n\phi}}{(1+\omega'^2)\epsilon_q}\right)\right) := \lambda_0\left(1 - \frac{R}{R_{c0}}\right), \tag{34}$$

where R_{c0} is the threshold of the standard model. Besides the two control parameters R and ω', Eq. (32) contains two parameters describing the migration and recombination effects,

$$\tilde{\alpha}^2 = \frac{\alpha^2 s_1(\gamma)}{P_1\pi^2} = \frac{\mu_\perp^+\mu_\perp^-\gamma_1\pi^2}{\sigma_a d^2}, \tag{35}$$

$$\tilde{r} = \frac{2r}{P_1} = \frac{\tau_d^{(0)}}{\tau_{rec}}. \tag{36}$$

The coupling of the director to the conductive mode is proportional to the square of an effective mobility parameter $\tilde{\alpha}$ which is α with μ and τ_q replaced by the geometrical means of $\mu_\perp^\pm$ and τ_q, τ_d, respectively. Experimentally $\tilde{\alpha}$ can be influenced by varying $\sigma_\perp d^2$, see Table III.

The growth rate of modes $\propto e^{\lambda t}$ in (32) is given by

$$\lambda = \frac{\lambda_\sigma + \lambda_n}{2} \pm \sqrt{\frac{(\lambda_\sigma - \lambda_n)^2}{4} - C^2\left(\frac{R\tilde{\alpha}}{1+\omega'^2}\right)^2} \tag{37}$$

$$C^2 = \frac{\epsilon_q^2\left(1 - \frac{\epsilon_a}{\epsilon_q}\frac{\sigma_q}{\sigma_a}\right)\left(1 - \frac{\epsilon_a}{\epsilon_q}L_{nn}q^2\right)}{\sigma_q^2(1 - L_{nn})}, \tag{38}$$

where C is (apart from a weak q dependence via $q_c(\omega')$) a fixed constant for a given NLC. For MBBA $C^2(q = q_c) = 1.19$ with $q_c = 1.51$ for $\omega' << 1$ and $C^2(q = q_c) = 2.71$ with

$q_c \to \infty$ for $\omega' \to \omega'_{cutoff}$. Setting $\epsilon_a = 0$ to simulate the material I52, see [9], one has $C^2 = 0.91, q_c = 1.21$, independent of frequency (in this approximation).

A Hopf bifurcation is characterized by a nonzero imaginary part of λ at threshold, $\mathrm{Re}\lambda(R_c, q_c) = 0$, $\mathrm{Im}\lambda(R_c, q_c) = \omega_H \neq 0$ with

$$\omega_H = 2\pi f_H = \frac{R_c \tilde{\alpha} C}{1+\omega'^2}\sqrt{1 - \frac{1}{C^2}\left(\frac{\tilde{r}}{\tilde{\alpha}}\frac{1+\omega'^2}{R_c} + \tilde{\alpha}\frac{\epsilon_{q_c}}{\sigma_{q_c}}\right)^2}. \tag{39}$$

The Hopf condition, namely, that the root be positive, leads essentially to conditions for $\tilde{r}/\tilde{\alpha}$ and $\tilde{\alpha}$. For typical material and system parameters (see Tables II and III), one usually has $\tilde{\alpha}\epsilon_q/(\sigma_q C) << 1$ so we are left with an upper limit for the recombination rate,

$$\tilde{r} < \frac{\tilde{\alpha} R_c C}{1+\omega'^2}. \tag{40}$$

Since $\tilde{r}/\tilde{\alpha} \propto (\sigma_\perp d^2)^{3/2}$ (Table III) this condition gets weaker for thinner and cleaner cells; for materials with $\epsilon_a < 0$ it is always fulfilled near the cutoff frequency ω'_{cutoff}, where $R_c \to \infty$. In the special case $\epsilon_a \to 0$, relevant for experiments with the nematic material I52 [9], Eq. (39) simplifies to

$$2\pi f_H(\epsilon_a = 0) = -\lambda_0\tilde{\alpha}\sqrt{(1-L_{nn}) - \left(\frac{-\tilde{r}}{\lambda_0\tilde{\alpha}} + (1-L_{nn})\tilde{\alpha}\right)^2} \tag{41}$$

If the Hopf conditions are well satisfied, the Hopf frequency is essentially $2\pi f_H = -\lambda_0\tilde{\alpha}(1-L_{nn})^{1/2}$ proportional to $\sigma_\perp^{-1/2} d^3$. For MBBA parameters with ϵ_a changed to zero (I52) this is in physical units $f_H \tau_d \approx 0.4\tilde{\alpha}$.

5. DISCUSSION

We presented a new theory for electroconvection by replacing the ohmic conductivity of the standard model with drift and diffusion of two species of charge carriers. The conductivity itself becomes a new dynamically active variable, if the recombination time is not small compared to the charge or the director relaxation time. We demonstrated by a simple analytical calculation that this new degree of freedom leads generically to a Hopf bifurcation, if the ratio $\tilde{\alpha}/\tilde{r}$ of the mobility parameter $\tilde{\alpha}$ and the recombination parameter $\tilde{r}$ is large enough.

Since the ratio $\tilde{\alpha}/\tilde{r}$ is proportional to $(\sigma_\perp d^2)^{-3/2}$, the above Hopf condition is fulfilled for thin and pure (small conductivity $\sigma_\perp$) samples, in qualitative agreement with experiments on MBBA, where Hopf is only found for thin [6, 8] and clean cells [23], and with experiments

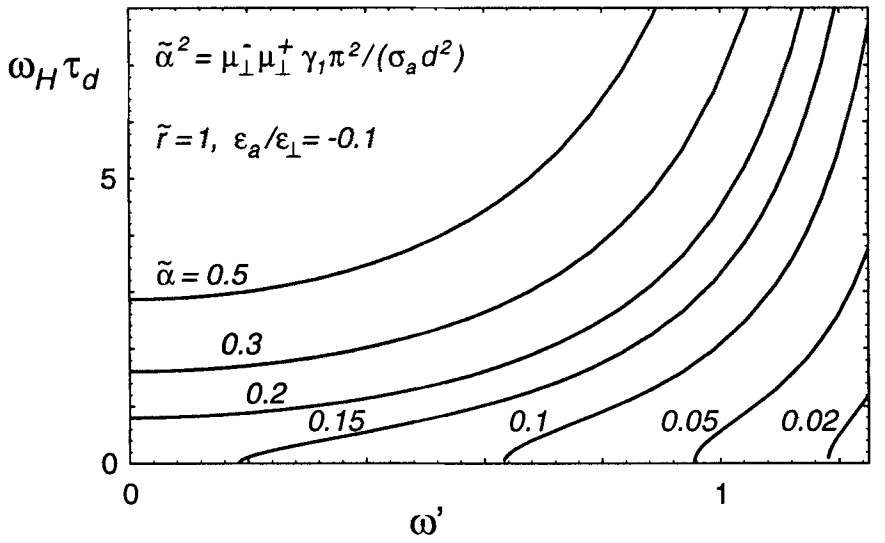

Figure 1: Hopf frequency $\omega_H = 2\pi f_H$, normalized to the director relaxation time, as function of the normalized external frequency $\omega' = \omega_{ext}\tau_q\epsilon_q/\sigma_q$ for the analytical model of Sec.4 with MBBA I parameters and $\tilde{r} = \tau_d/\tau_{rec} = 1$. $\tilde{\alpha}$ is the mobility parameter. The cutoff frequency corresponds to $\omega' = 1.4$.

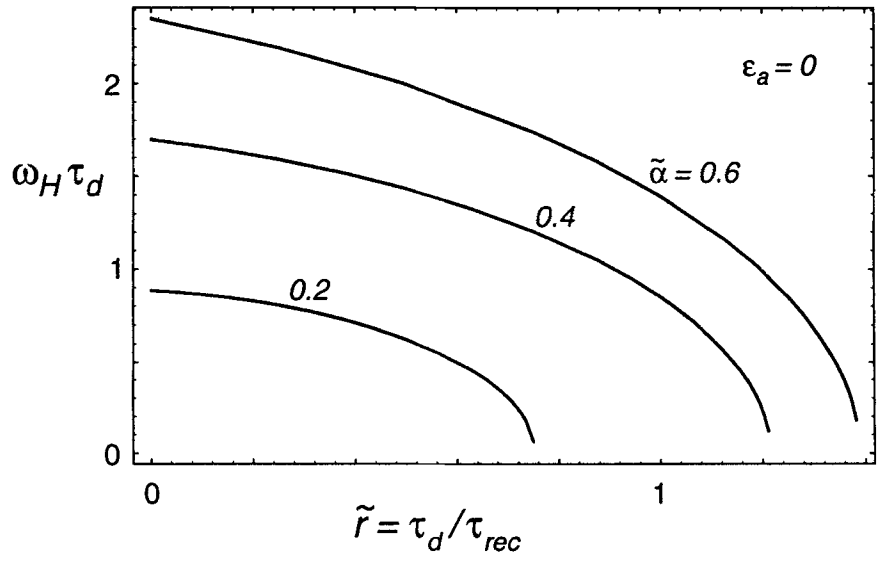

Figure 2: Hopf frequency as function of the recombination rate for MBBA I parameters with ϵ_a set to zero (to simulate *I*52) and different values of $\tilde{\alpha}$.

on I52 [9] where the conductivity could be changed and Hopf was found only for low conductivities. For materials with $\epsilon_a < 0$ (e.g. MBBA) the Hopf condition gets weaker (and, if it is fullfilled, the Hopf frequency increases) with increasing external frequencies ω_{ext}. For $\epsilon_a = 0$ the Hopf condition is nearly independent of ω_{ext}. In fact in I52, Hopf is observed in sufficiently clean samples for all frequencies [9].

In Fig.1 our results for the (normalized) Hopf frequency as a function of the (normalized) external frequency are plotted for MBBA for various values of $\tilde{\alpha}$ and $\tilde{r} = 1$. The behavior found in the experiments of ref.[6] is similar to our results for $\tilde{\alpha} \approx 0.1$ (at $\tilde{r} = 1$), whereas the behavior found in ref.[8] is quite similar to our results for $\tilde{\alpha} \approx 0.17$. Figure 2 shows the Hopf frequency as a function of $\tilde{r}$ for MBBA with $\epsilon_a = 0$ for three values of $\tilde{\alpha}$.

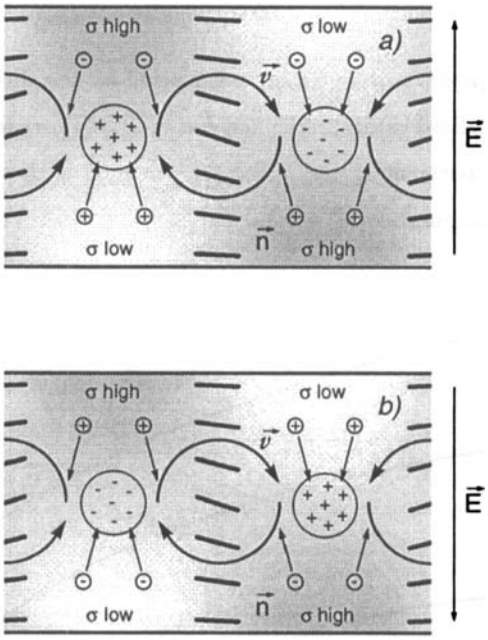

Figure 3: Sketch of the spatial distribution of the physical quantities inside the nematic layer (conductive regime). The straight arrows indicate the contributions to the current carried by each species. The shading illustrats the conductivity mode (dark = σ high, light = σ low)

A qualitative understanding of the mechanism leading to the Hopf bifurcation can be obtained by noting that the conductivity mode describing rearrangement of the total charge carrier density (each species weighed by its mobility) on the time scale of τ_{mig} reduces the charge density produced by the standard Carr-Helfrich charge focussing mechanism. This antagonistic cross coupling of σ and ρ can already be identified in Eqs.(8),(9) or (14), (15) (one may choose e.g. equal mobilities, $\gamma = 1$, so that for $D = 0, r = 0$ one is left only with cross-coupling terms), and carries through to Eqs.(32), where it is easily seen to lead to an increase of the threshold (note that in Eqs.(32) all effects from the standard theory are included in the relaxation rate λ_n). Figure 3 gives a sketch of the resulting distribution of the physical quantities inside the layer at two instances separated by half of an external period. If the time scale of the cross coupling effect is sufficiently long, the system acts like a spring and destabilization occurs in an oscillatory manner. The linear modes of the system then describe left and right traveling rolls (or "waves"), although in principle one could also have the more complicated superposition to standing waves.

Since we made crude approximations (adiabatic elimination of the charge, trivial basic state, lowest-order Galerkin expansion, normal-roll state also for I52) we can expect the above predictions to agree only qualitatively with the experiments. Calculations with the full basic state and linear equations are planned in the future. Then it should be possible, to determine the recombination rate constant and the mobility ratio of the two species by a fit of the predicted Hopf frequency to the measured one. To get information about the basic state one can compare the predicted cell impedance with measurements. A weakly nonlinear analysis of the new model should determine the parameter ranges where the predicted Hopf bifurcation is continuous or hysteretic. Finally one should be able to compute all parameters of the universal Ginzburg-Landau description valid near threshold.

We wish to thank A. Hertrich and W. Pesch for helpful discussions, M. Dennin for making available his experimental results prior to publication, and A. Buka for a critical reading of the manuscript. One of us (M.T.) is grateful to the Arizona Center for Mathematical Sciences at Tucson, where part of this work was performed, for its hospitality. Financial support by Deutsche Forschungsgemeinschaft (SFB 213, Bayreuth) and Stiftung Volkswagenwerk is gratefully acknowledged.

References

[1] E. Bodenschatz, W. Zimmermann and L. Kramer, J. Phys. France **49**, 1875 (1988);

L. Kramer, E. Bodenschatz, W. Pesch, W. Thom and W. Zimmermann, Liquid Cryst. **5**, 699 (1989).

[2] W. Zimmermann in *Nematics: Mathematical and Physical Aspects*, J.-M. Coron, J.M. Ghidaglia, and F. Helein, eds., NATO ASI Series C - Vol.332 (Kluwer Acad. Publishers, Dordrecht, 1991), pp.401.

[3] I. Rehberg, B.L. Winkler, M. de la Torre Juarez, S. Rasenat, and W. Schöpf, *Festkörperprobleme-Advances in Solid-State physics* **29**, 35 (1989).

[4] L. Kramer and W. Pesch, *Convective Instabilities in Nematic Liquid Crystals*, to appear in *Annual Review of Fluid Mechanics***27**, 1995.

[5] S. Kai and K. Hirakawa, Prog. Theor. Phys. Suppl. **64**, 212 (1978).

[6] I. Rehberg, S. Rasenat, and V. Steinberg, Phys. Rev. Lett **62**, 756 (1989).

[7] A. Joets and R. Ribotta, Phys. Rev. Lett. **60** 2164 (1988).

[8] I. Rehberg, S. Rasenat, J.Fineberg, M. de la Torre and V. Steinberg, Phys. Rev. Lett **61**, 2449 (1988).

[9] M. Dennin, D.S. Cannell, and G. Ahlers, this proceedings.

[10] I. Rehberg, S. Rasenat, M. de la Torre Juarez, W. Schöpf, F. Hörner, G. Ahlers, and H.R. Brand, Phys. Rev. Lett **67**, 596 (1991).

[11] Ericksen, J. L., Arch. Ration. Mech. Analysis **23**, 266 (1966).

[12] F. M. Leslie, Quart. J. Mech. Appl. Math. **19**, 357 (1966).

[13] R. Chang and J.M. Richardson, Mol. Cryst. Liq. Cryst **28**, 189 (1973).

[14] R.J. Turnbull, J. Phys. **D6**, 1745 (1973).

[15] H. Naito, K. Yoshida, and M. Okuda, J. Appl. Phys **73**, 1119 (1993).

[16] H. Naito, M. Okuda, and A. Sugimura Phys. Rev. **A44**, 3434 (1991).

[17] A.Sugimura et al., Phys. Rev. **B43**, 8272 (1991).

[18] S. Murakami, H. Naito, M. Okuda, and A. Sugimara, Presented (Poster K-P23) at the 15th ILCC in Budapest, 1994.

[19] N. Felici, Revue generale de l' electricite **78**, 717 (1969).

[20] M. Treiber and L. Kramer, Phys. Rev. **E94**, 3184 (1994).

[21] D. Diguet et al., Compt. Rend. **271B**, 954 (1970)

[22] A.T. Perez and A. Castellanos, Phys. Rev. **A40**, 5844 (1989).

[23] H. Richter, A. Buka and I. Rehberg, "Convection in a Homeotropically Aligned Nematic", to be published (homeotropically aligned specimens with $\epsilon_a < 0$ behave in many respects similar to planarly aligned ones).